11th International Workshop on Ship and Marine Hydrodynamics
Hamburg, Germany, September 22-25, 2019

Flow Visualization of Horseshoe Vortices around a Surface-Mounted Hydrofoil

Chun-Yao Yang, Yaw-Huei Lee, Yi-Chih Chow*

National Taiwan Ocean University, Department of Systems Engineering and Naval Architecture
2 Pei-Ning Road, Keelung 20224, Taiwan

*ycchow@email.ntou.edu.tw

ABSTRACT

The horseshoe vortex (HSV) usually induces undesirable effects like noise, vibration, and drag. Therefore, the HSV is not only of academic interest but also a critical engineering issue. We used two high-speed cameras with prolonged exposure time to record the pathlines of the seeding particles illuminated by a continuous-wave laser. These particle pathlines constitute a very clear visualization of flow coherent structures, especially vortical structures, i.e. vortices. Next, we used this PIV-based flow visualization technique to study the kinematics of HSV as a coherent structure associated with a surface-mounted NACA66 hydrofoil for a Reynolds number of 8,820 (based on the maximum thickness of the hydrofoil and the free-stream velocity).

We observed six kinematic patterns of HSV, and measured the occurrence probability for each pattern: (i) steady (17%), (ii) amalgamating (26%), (iii) breakaway (31%), (iv) transition (12%), (v) random (8%), and (vi) roll-up (6%). The naming and definitions of patterns (i) to (v) are adopted from Younis et al [1]. We also found that the HSV adjacent to the hydrofoil surface rises as it extends downstream.

1 INTRODUCTION

Many juncture flow phenomena exist in nature and in engineering applications. These vortical flows are generated in the front junction of a surface-mounted obstacle and form a horseshoe shape structure extending far downstream. This is why it was named “horseshoe vortex” (HSV). It is commonly observed when a flow passes by a surface-mounted obstacle mainly because of the incoming separated boundary layer and the strong adverse pressure gradient induced by the obstacle in the approaching flow direction. The HSV is a complicated three-dimensional vortical flow, which not only wraps around the obstacle but also influences flow characteristics from the upstream to the downstream region of the obstacle. The HSV usually induces undesirable effects like noises, vibration, and drag in many engineering applications. For instance, the HSV is an important issue of scouring, which threatens the safety of bridges [2, 3]; the behaviour of the HSV generated at the sail-body junction of a submarine results in an influence on the uniformity of the hull wake flow into the propeller, increasing the unsteady blade loading and generating significant noise [4-6]. In turbomachinery applications, the HSV has been found to increase local heat transfer rates in leading-edge regions of blades, causing thermal mechanical fatigue [7]. Therefore, the HSV is not only of academic interest but also a critical engineering issue.

Many previous publications mainly examined the flow characteristics of HSV and their trends with parameters such as model geometries (shape or size), boundary layer thickness, and Reynolds number. Schwind [8] used the method of smoke flow visualization to qualitatively study the flow behaviour of HSV at the junction of a wedge cylinder mounted on the surface in a wind tunnel. He categorized the flow patterns of HSV into five different regimes, which showed a trend that the number of HSV increases with the Reynolds number. Thomas [9] performed smoke-wire visualizations to explore the effect of aspect ratio (height/diameter, H/D) on the development of HSV upstream a circular cylinder mounted on a plate in a wind tunnel. Chou and Chao [10] studied the branching behaviour of HSV upstream of rectangular cylinders with a series of widths in a water tunnel with colored-dye visualization. The results indicated, with the

increasing width of the rectangular cylinder, the structure of HSV is transformed from one conventional HSV into a wavy structure, and then branches into steady smaller U-shape vortices of odd numbers. Hu et al [11] used the Particle Image Velocimetry (PIV) technique to study the topology of HSV in front of various surface-mounted obstacles (equilateral triangle, 2:1 ellipse, circle, 1:2 ellipse and square) in a water tunnel. The results indicated that the boundary layer thickness, width of the obstacle and the effect of the model bluntness play a vital role in the topological transition. The number and size of HSV increased as the bluntness increased. In addition, as the width of obstacle increases, the HSV splits into smaller vortices, corresponding to the results obtained by Chou and Chao [10]. Wei et al. [12] investigated the influence of the cylinder section shape on the flow characteristics of HSV with the smoke-wire, Laser Induced Fluorescence (LIF), surface pressure and Laser Doppler Velocimeter (LDV), and showed that the correlation between the frontal bluntness of the cylinder and the suppression of the HSV due to the reduction of the adverse pressure gradient. The flow visualization experiments regarding the possible effect of cylinder aspect ratio on the HSV appearing at the junction of a short cylinder and a pair of flat parallel plates were conducted with the PIV technique by Rodríguez y Domínguez et al. [13, 14], who discovered that the behaviour of HSV becomes independent of the cylinder height for sufficiently tall cylinders (aspect ratio, $H/D > 1.0$). Besides, Sahin et al. [15], Ozturk et al. [16] and El Hassan et al. [17] paid attention to the effect of HSV on the wake of surface-mounted obstacles.

Some studies focused on the kinematic behaviours of HSV as a coherent structure and qualitatively classified them into several kinematic patterns. Baker [18] experimentally investigated the HSV formed around a circular cylinder using smoke flow visualization in a wind tunnel. The visualization showed three different kinds of HSV system with increasing Reynolds number: steady HSV, regular oscillatory HSV and irregular unsteady HSV. Wei et al. [19] performed experiments to study the flow structure of HSV upstream of a short cylinder (prism, square and circular geometry) mounted on a flat plate in a water tunnel with visualization techniques such as the LIF and the smoke-wire. The flow visualization results indicated that the configuration of the HSV in the range of Reynolds number from 1,000 to 32,000 could be classified into four basic flow patterns as steady HSV system ($Re < 2000$), periodically oscillating HSV system ($2000 < Re < 5000$), unsteadily oscillating HSV system ($5000 < Re < 8000$) and turbulent juncture flow ($Re > 8000$). Lin et al. [20, 21] conducted a series of experiments with the PIV technique to study the flow behaviour of HSV in front of a vertical plate mounted on a plate in a water channel. The kinematic patterns of HSV were classified into four types: steady HSV, periodic oscillation vortex system with small displacement, periodic breakaway vortex and irregular vortex system. They provided the detailed information concerning the connections between HSV patterns and several experimental parameters based on the boundary layer thickness, Reynolds number and aspect ratio (height/width). Rodríguez y Domínguez et al. [13, 14] also discovered five different flow regimes of HSV in the experiments: steady, oscillatory, amalgamating, breakaway and chaotic vortex systems.

Most of the previously reported studies have focused on studying the features of HSV upstream of the models that were nearly all circular, rectangular, triangle or ellipse cylinders. However, the study of HSV upstream a hydrofoil cylinder receives less attention. Moreover, the data obtained with the experimental methodologies adopted by previous studies are somewhat not very straightforward to human eyes, i.e. not completely visualized. Therefore, we aimed at establishing a flow visualization technique based on the PIV principles and then studying the kinematics of HSV upstream a surface-mounted hydrofoil in a low speed water tunnel.

2 EXPERIMENTAL APPARATUS AND METHOD

2.1 Water Tunnel and Experimental Model

Qualitative flow visualization was carried out at a free-stream velocity $U=0.21$ m/s in a low speed and open-top water tunnel at the Particle Image Velocimetry Laboratory of the Department of System Engineering and Naval Architecture, National Taiwan Ocean University. As shown in Figure 1 (a), the test section of the water tunnel was rectangular with the length, width, and height of 124, 25, and 25 cm, respectively. In order to acquire the qualitative experimental results, both sides and bottom of the water tunnel were equipped with three transparent glass windows to be beneficial for the PIV-based visualization method. A surface-mounted NACA66 hydrofoil, as shown in Figure 1 (b), vertical to the bottom of the water tunnel is used as the experimental model with the chord length, maximum thickness (d), and height of 20, 4.2,

and 17.5 cm, respectively. The leading edge of the vertical foil cylinder is placed in the middle along the centerline of the water tunnel.

(a) (b)

Figure 1: (a) Low speed water tunnel; (b) Surface-mounted NACA66 hydrofoil cylinder

2.2 Flow Visualization

The PIV-based flow visualization technique was employed to observe the flow coherent structure of HSV around a surface-mounted hydrofoil, which included several main components: (1) light source: a 5-watt Diode-Pumped Solid-State continuous-wave laser (green light, wavelength 532 nm); (2) laser optics; (3) seeding particles: hollow glass spheres (10 μm diameter); (4) digital camera: two high speed CMOS cameras (Phantom v310, 1280x800 pixels). The coordinate system (X, Y, Z) adopted is shown in Figure 2. The inflow direction was in the -X direction. The coordinate Y and Z were in the transverse and spanwise directions.

The experimental procedure is described below. First, we used two high-speed cameras with prolonged exposure time to record the pathlines of the seeding particles illuminated by a continuous-wave laser. These particle pathlines constitute a very clear visualization of flow coherent structures, especially vortical structures, i.e. vortices. Next, we used this PIV-based flow visualization technique with one vertical (X-Y plane) and one horizontal (X-Z plane) laser light sheets simultaneously generated to study the kinematics of HSV associated with a surface-mounted NACA66 hydrofoil for a Reynolds number of 8,820 (based on the maximum thickness of the hydrofoil and the free-stream velocity), as shown in Figure 2.

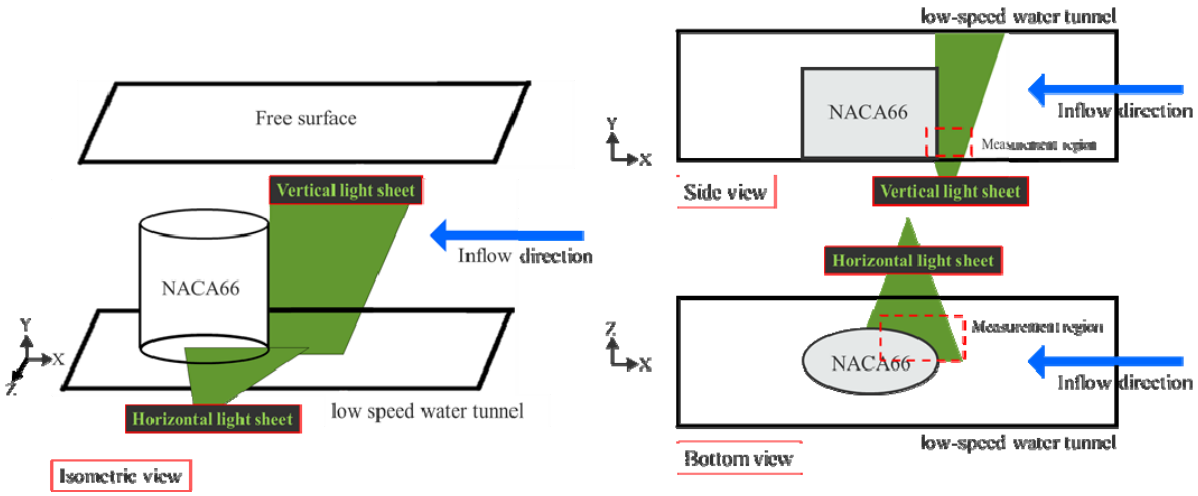

Figure 2: Schematic diagram of the PIV-based flow visualization technique with the synchronized generation of dual laser light sheets applied on the HSV problem associated with a surface-mounted NACA66 hydrofoil.

3 RESULTS AND DISCUSSION

3.1 Classification and Occurrence Probability of Kinematic Pattern of HSV

The flow regimes of HSV studied in different ranges of Reynolds numbers with various shape of models by Wei et al. [12], Lin et al. [20, 21], Rodríguez y Domínguez et al. [13, 14] and Younis et al. [1] were completely complicated. Obviously, at the same size and shape of model, the flow regimes of HSV developed around the model were changed highly dependent on the Reynolds numbers. In contrast to previous studies, we discover all six kinematic patterns of HSV occurred in front of a surface-mounted NACA66 hydrofoil merely at one Reynolds number of 8,820, which are: (i) steady, (ii) amalgamating, (iii) breakaway, (iv) transition, (v) random, and (vi) roll-up. The naming and definitions of patterns (i) to (v) are adopted from Younis et al. [1]. The last one, (vi) roll-up, has never been reported in previous publications to the authors' best knowledge.

From Figure 3 to Figure 8, the vertical boundary (X=0 mm), on the left side of these pictures, indicates the leading edge of the NACA66 hydrofoil, and the bottom boundary (Y=0 mm) denotes the surface of the low speed water tunnel. The direction of the inflow is from the right side to the left side. Using the flow visualization with the vertical light sheet, the detailed illustrations of six kinematic patterns of HSV are described below.

(i) Steady

The HSV in steady pattern means that the HSV is maintained at the same position with no observable displacement or oscillation of the vortex structure in time.

As shown in Figure 3, three discrete primary vortices (labelled V1, V2 and V3) exist respectively at X_{V1}=11 mm, X_{V2}=15 mm and X_{V3}=4 mm near the surface of the low speed water tunnel at the initial time t= 0.00s. As time proceeds (t=0.50s), the centre position of V1 vortex remains nearly unchanged at X_{V1}=11 mm during this time.

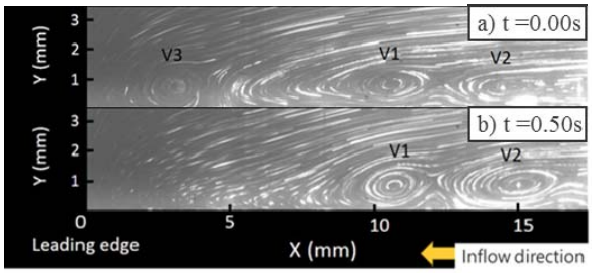

Figure 3: Time series of image visualizing the steady process of vortex.

(ii) Amalgamating

The HSV in amalgamating pattern means that two discrete HSVs amalgamate with each other and eventually forms a new HSV.

As shown in Figure 4, two primary vortices(labelled V1, V2) and one secondary vortex(labelled V3) exist respectively at X_{V1}=11 mm, X_{V2}=16 mm and X_{V3}=13 mm near the surface of the low speed water tunnel at the initial time t=0.00s. From t=0.00s to t=0.33s, V1 vortex moves toward downstream and catches up with V3 vortex. At the last instant (t=0.50s), V1 vortex and V2 vortex are combined to form a new V1* vortex.

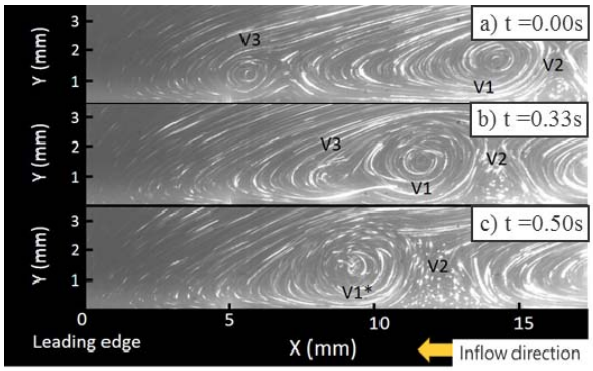

Figure 4: Time series of image visualizing the amalgamating process of vortex.

(iii) Breakaway

The HSV in breakaway pattern means that the HSV splits from the upstream and moves toward the obstacle, as the HSV advances close to the juncture of the obstacle and the surface where the size and structure of HSV gradually becomes smaller and collapsed due to vortex stretching until the HSV becomes detached and moves away downstream.

As shown in Figure 5, the presence of two primary vortices(labelled V1, V2) and one secondary vortex(labelled V3) are respectively located at X_{V1}=11 mm, X_{V2}=16 mm and X_{V3}=13 mm near the surface of the low speed water tunnel at the initial time t=0.00s. As time passes by (t=0.42s), the V1 vortex approaching to the leading edge rapidly reduces its size at the X_{V1}=2 mm. Later (t=0.50s), V1 vortex completely disappears in front of the leading edge at last.

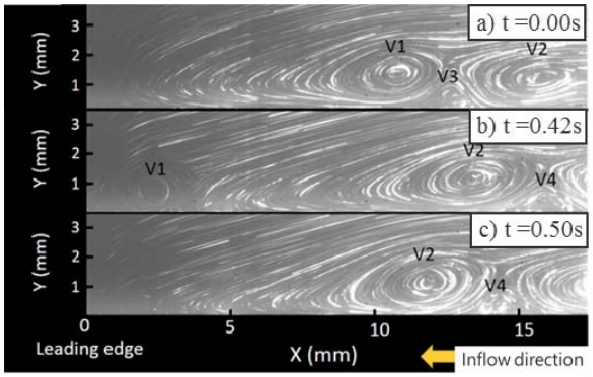

Figure 5: Time series of image visualizing the breakaway process of vortex.

(iv) Transition

The HSV in transition pattern means that the HSV firstly breaks away from the upstream toward the leading edge, but, before the HSV detached toward downstream in the corner, the upstream HSV with strong attraction pulls the corner HSV back, and, eventually, both of them are amalgamated into a newly formed HSV.

As shown in Figure 6, there are two primary vortices (labelled V1, V2) and one secondary vortex (labelled V3) existing respectively at X_{V1}=7.5 mm, X_{V2}=16.5 mm and X_{V3}=10 mm near the surface of the low speed water tunnel at the initial time t=0.00s. During the time interval (t=0.00s to t=0.33s), V1 vortex is moving in the down until V1 vortex reaches the leftmost position at X_{V1}=5 mm. Finally, at t=0.50s, V1 vortex and V2 vortex start to merge with each other.

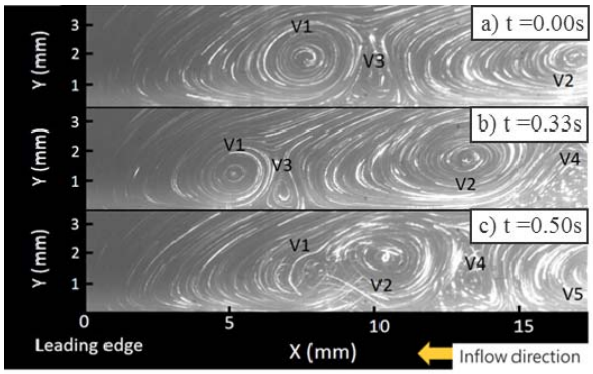

Figure 6: Time series of image visualizing the transition process of vortex.

(v) Random

The HSV in random pattern means that the flow field become so extremely disordered that there is no recognizable kinematic pattern. No sustaining coherent structures can be found in this pattern.

As shown in Figure 7, only one primary vortices (labelled V1) can be clearly seen at X_{V1}=11 mm near the surface of the low speed water tunnel at the initial time t=0.00s. Starting from t=0.00s to t=0.50s, the flow field presents a large area of chaotic irregularity and the structure of HSV became distorted in the flow domain.

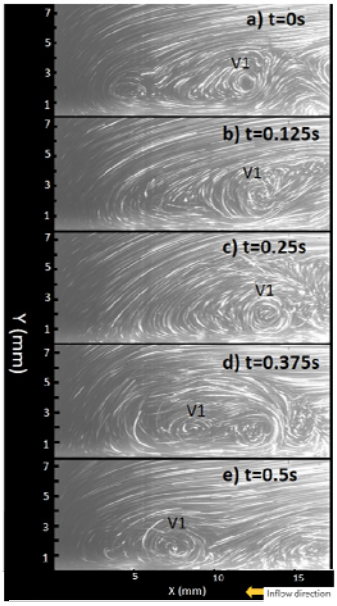

Figure 7: Time series of image visualizing the random process of vortex.

(vi) Roll-up

The HSV in roll-up pattern means that the flow field is rolling up to form a new primary vortex at the junction of the NACA66 hydrofoil where no vortex exists in the beginning.

As shown in Figure 8, only two discrete primary vortices (labelled V1 and V2) can be observed respectively at X_{V1}=10.6 mm and X_{V2}=15.5 mm at the initial time t=0.00s. At a later instant (t=0.17s), a primary vortex (labelled V3) forms suddenly in front of the leading edge at X_{V1}=5.6 mm.

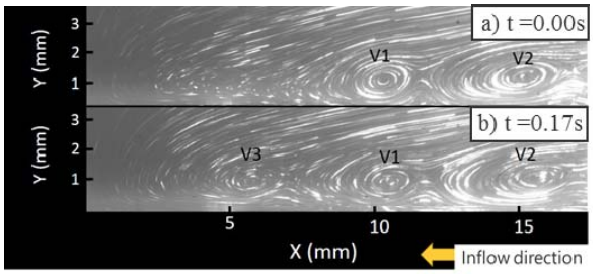

Figure 8: Time series of image visualizing the roll-up process of vortex.

Using the flow visualization with the vertical light sheet, we discovered six kinematic patterns of HSV, and then counted the number of occurrences of every and each pattern to calculate the occurrence probability for each pattern. The results of occurrence probability of kinematic pattern of HSV are: (i) steady (17%), (ii) amalgamating (26%), (iii) breakaway (31%), (iv) transition (12%), (v) random (8%), and (vi) roll-up (6%). The minimum occurrence probability of kinematic pattern of HSV is the roll-up pattern, which may be one of the reason why it has never been reported in previous publications to the authors' best knowledge.

3.2 Method of HSV Identification in the Horizontal Light Sheet

For the flow visualization with the horizontal light sheet (X-Z plane), we developed an analysis method to identify the locations of HSV and determine the vertically moving direction of HSV. From the observation of the flow visualization with the vertical light sheet in front of the NACA66 hydrofoil as mentioned previously, we know that the height of the center of the HSV is slightly between 1 mm and 2 mm. Therefore, the vertical height of the horizontal light sheet with a thickness of 1 mm is set at Y=1.5 mm. When different position of the HSV is illuminated by the horizontal light sheet at a fixed height, the particle pathline of the HSV region will exhibit various flow direction types due to its three-dimensional rotational motion. As shown in the sectional view (YZ plane) of the HSV in the Figure 9 (b), only the upper part of the HSV intersects with the light sheet. From the bottom view (XZ plane) in the Figure 9 (c), the particle pathlines in the HSV region move in a certain oblique direction from the upper left side to the lower right side (as red line direction), but the particle pathlines in the surrounding free-stream region smoothly move downstream (as yellow line direction). As shown in the sectional view (YZ plane) of the HSV in the Figure 10 (b), only the middle part of the HSV intersects with the light sheet. From the bottom view (XZ plane) in the Figure 10 (c), the particle pathlines in the HSV region move in alternating direction (as red line direction), but the particle pathlines in the surrounding free-stream region smoothly move downstream (as yellow line direction). As shown in the sectional view (YZ plane) of the HSV in the Figure 11 (b), only the lower part of the HSV intersects with the light sheet. From the bottom view (XZ plane) in the Figure 11 (c), the particle pathlines in the HSV region move in a certain oblique direction from the upper right side to the lower left side (as red line direction), but the particle pathlines in the surrounding free-stream region smoothly move downstream (as yellow line direction).

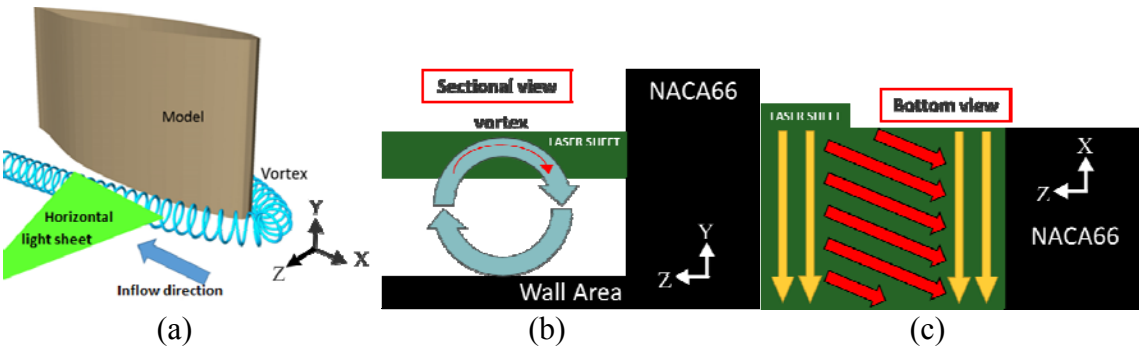

Figure 9: Sample orthographic views with the horizontal light illuminating the upper part of HSV. (a) Pictorial view; (b) Sectional view; (c) Bottom view (the red lines indicating the moving direction of the

particle pathlines in the HSV region; the yellow lines indicating the moving direction of the particle pathlines in surrounding free-stream region).

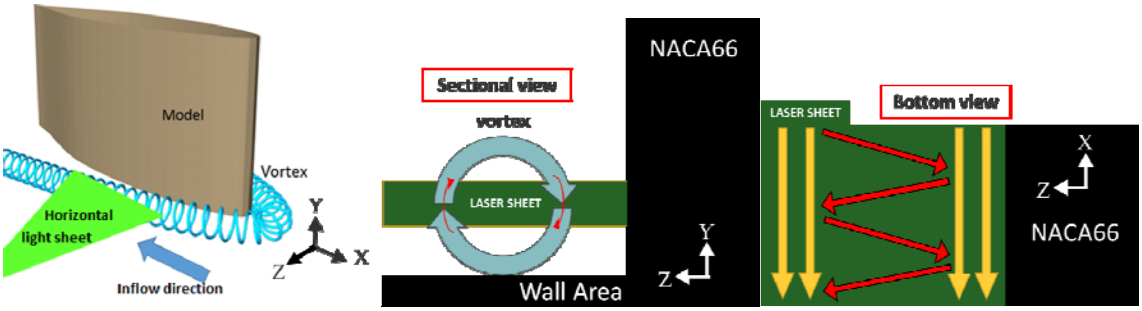

(a) (b) (c)

Figure 10: Sample orthographic views with the horizontal light illuminating the middle part of HSV. (a) Pictorial view; (b) Sectional view; (c) Bottom view (the red lines indicating the moving direction of the particle pathlines in the HSV region; the yellow lines indicating the moving direction of the particle pathlines in surrounding free-stream region).

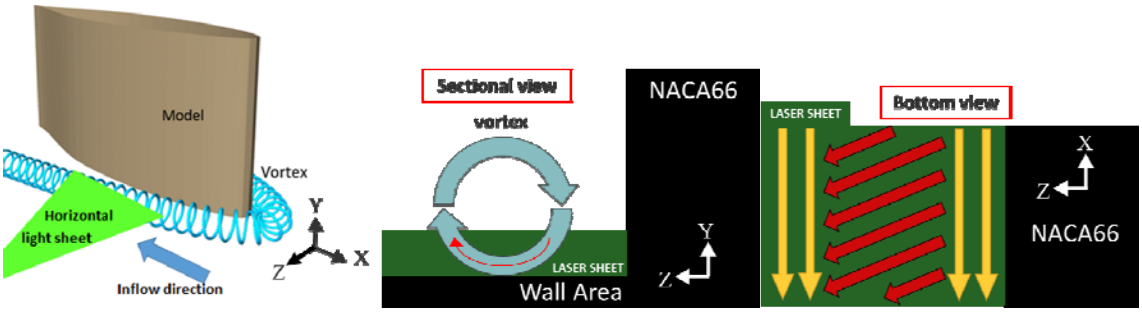

(a) (b) (c)

Figure 11: Sample orthographic views with the horizontal light illuminating the lower part of HSV. (a) Pictorial view; (b) Sectional view; (c) Bottom view (the red lines indicating the moving direction of the particle pathlines in the HSV region; the yellow lines indicating the moving direction of the particle pathlines in surrounding free-stream region).

As shown in Figure 12, two HSVs are identified in the image recorded by the high-speed camera from the bottom of the water tunnel, and outlined by two red solid lines. Near the leading edge (labelled as L.E.) of the NACA66 hydrofoil, the particle pathlines move in a certain oblique direction from the upper left side to the lower right side between two red solid lines, demonstrating that the upper part of the HSVs are intersecting with the horizontal light sheet. However, the particle pathline pattern between two red solid lines changes from moving in alternating direction to moving in a certain oblique direction from the upper right side to the lower left side in the downstream, pointing that the HSV adjacent to the hydrofoil surface rises as it extends downstream.

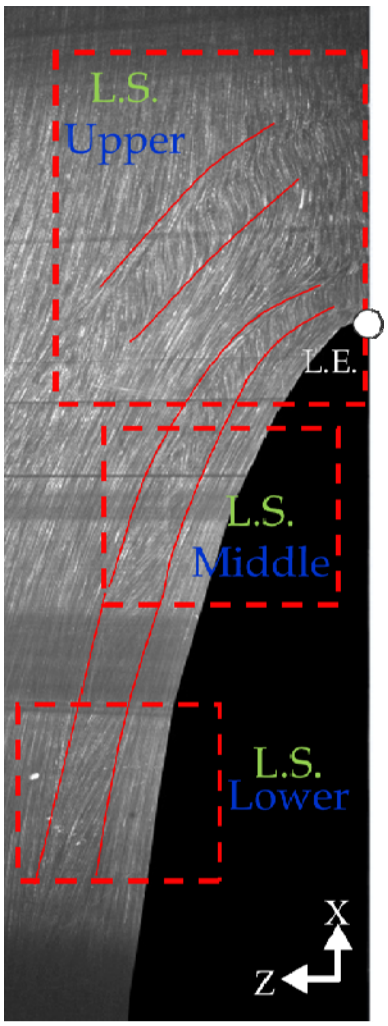

Figure 12: Flow visualization with the horizontal light sheet (denoted as L.S., and the blue words Upper, Middle and Lower indicating the position of the HSV where the light sheet intersects). Two HSVs are identified in the image and outlined by two red solid lines.

4 CONCLUSION

In order to study the HSV associated with a surface-mounted NACA66 hydrofoil for a Reynolds number of 8,820 (based on the maximum thickness of the hydrofoil and the free-stream velocity), we established a flow visualization technique based on PIV principles to study the kinematics of HSV as a coherent structure. Two high-speed cameras with prolonged exposure time to record the pathlines of the seeding particles illuminated by a continuous-wave laser were used to conduct experiments. The experimental results were divided into two parts according to the measurement area with one vertical (X-Y plane) and one horizontal (X-Z plane) laser light sheets simultaneously generated.

Using the flow visualization with the vertical light sheet in front of the leading edge of the NACA66 hydrofoil, we observed six kinematic patterns of HSV, and then counted the number of occurrences of every and each pattern to calculate their occurrence probabilities. The results are: (i) steady (17%), (ii) amalgamating (26%), (iii) breakaway (31%), (iv) transition (12%), (v) random (8%), and (vi) roll-up (6%). It is clearly evident that the breakaway is the most frequent event (pattern) for the HSV. The roll-up pattern has never been reported in previous publications to the authors' best knowledge.

For the flow visualization with the horizontal light sheet at a fixed height of Y=1.5 mm, we developed an analysis method to identify the locations of HSV and determined the vertically moving direction of HSV. We found that the HSV lifts up from the ground as it extends downstream.

REFERENCES

[1] Younis, M.Y., H. Zhang, B. Hu, Z. Muhammad and S. Mehmood. “Investigation of different aspects of laminar horseshoe vortex system using PIV”. In: *Journal of Mechanical Science and Technology*, Vol. 28 (2014), 527-537.

[2] Chiew, Y.M. and B.W. Melville. “Local scour around bridge piers”. In: *Journal of Hydraulic Research*, Vol. 25 (1987), 15-26.

[3] Muzzammil, M., T. Gangadharaiah and A.K. Gupta. “An experimental investigation of a horseshoe vortex induced by a bridge pier”. In: *Proceedings of the Institution of Civil Engineers: Water Management*, Vol. 157 (2004), 109-119.

[4] Liu, Z.H., Y. Xiong, Z.Z. Wang, S. Wang and C.X. Tu. “Numerical simulation and experimental study of the new method of horseshoe vortex control”. In: *Journal of Hydrodynamics*, Vol. 22 (2010), 572-581.

[5] Jimnez, J.M. and A.J. Smits. “Tip and junction vortices generated by the sail of a yawed submarine model at low Reynolds numbers”. In: *Journal of Fluids Engineering*, Vol. 133 (2011).

[6] Liu, Z.H. and Y. Xiong. “The method to control the submarine horseshoe vortex by breaking the vortex core”. In: *Journal of Hydrodynamics*, Vol. 26 (2014), 637-645.

[7] Praisner, T.J. and C.R. Smith. “The dynamics of the horseshoe vortex and associated endwall heat transfer - Part II: Time-mean results”. In: *Journal of Turbomachinery*, Vol. 128 (2006), 755-762.

[8] Laboratory, M.I.o.T.G.T. and R.G. Schwind. “The Three Dimensional Boundary Layer Near a Strut”. Massachusetts Institute of Technology, Department of Mechanical Engineering, 1962.

[9] Thomas, A.S.W. “The unsteady characteristics of laminar juncture flow”. In: *Physics of Fluids*, Vol. 30 (1987).

[10] Chou, J.H. and S.Y. Chao. “Branching of a horseshoe vortex around surface-mounted rectangular cylinders”. In: *Experiments in Fluids*”. Vol. 28 (2000), 394-402.

[11] Hu, Bo, H. Zhang, M.Y. Younis, Y. Li and M.S. Raza. “Experimental investigation on the transition of separation/attachment in steady laminar juncture flows”. In: *Experiments in Fluids*, Vol. 56 (2015).

[12] Wei, Q. D., J.M.Wang, G. Chen, Z.B. Lu and W.T. Bi. “Modification of Junction Flows by Altering the Section Shapes of the Cylinders”. In: *Journal of Visualization*, Vol. 11 (2008), 115-124.

[13] Rodríguez y Domínguez, M., R. Romero-Méndez, M. Ramos-Paláu and F.G. Pérez-Gutiérrez. “The laminar horseshoe vortex upstream of a short-cylinder confined in a channel formed by a pair of parallel plates”. In: *Journal of Visualization*, Vol. 9 (2006), 309-318.

[14] Rodríguez y Domínguez, M., R. Romero-Méndez, F. De Lange Dirk and A. Hernández-Guerrero. “Laminar Horseshoe Vortices Upstream of a Short Cylinder Normal to a Flat Plate”. In: *Ingeniería Mecanica, Tecnología y Desarrollo*, Vol. 3 (2011), 219-228.

[15] Sahin, B., N.A. Ozturk and H. Akilli. “Horseshoe vortex system in the vicinity of the vertical cylinder mounted on a flat plate”. In: *Flow Measurement and Instrumentation*, Vol. 18 (2007), 57-68.

[16] Ozturk, N.A., A. Akcayoglu, and B. Sahin. “Downstream particle image velocimetry measurements of a circular cylinder-plate junction. Proceedings of the Institution of Mechanical Engineers, Part C”. In: *Journal of Mechanical Engineering Science*, Vol. 223 (2009), 1837-1849.

[17] El Hassan, M., J. Bourgeois, and R. Martinuzzi. “Boundary layer effect on the vortex shedding of wall-mounted rectangular cylinder”. In: *Experiments in Fluids*, Vol. 56 (2015).

[18] Baker, C.J. “The laminar horseshoe vortex”. In: *Journal of Fluid Mechanics*, Vol. 95 (1979), 347-367.

[19] Wei, Q.D., G. Chen and X.D. Du. “An Experimental Study on the Structure of Juncture Flows”. In: *Journal of Visualization,* Vol. 3, No. 4 (2001), 341-348.

[20] Lin, C., P.H. Chiu and S.J. Shieh. “Characteristics of horseshoe vortex system near a vertical plate-base plate juncture”. In: *Experimental Thermal and Fluid Science*, Vol. 27(2002), 25-46.

[21] Lin, C., T.C. Ho and S. Dey. “Characteristics of steady horseshoe vortex system near junction of square cylinder and base plate”. In: Journal of Engineering Mechanics, Vol. 134 (2008), 184-197.